Global phosphoproteomic profiling reveals perturbed signaling in a mouse model of dilated cardiomyopathy

Uros Kuzmanov[a,b,1], Hongbo Guo[a,1], Diana Buchsbaum[c], Jake Cosme[c], Cynthia Abbasi[c], Ruth Isserlin[a], Parveen Sharma[c], Anthony O. Gramolini[b,c,2], and Andrew Emili[a,2]

[a]Donnelly Centre for Cellular and Biomolecular Research, University of Toronto, Toronto, ON, Canada M5S 3E1; [b]Ted Rogers Centre for Heart Research, University of Toronto, Toronto, ON, Canada M5G 1M1; and [c]Department of Physiology, University of Toronto, Toronto, ON, Canada M5S 3E1

Edited by Christine E. Seidman, Howard Hughes Medical Institute, Harvard Medical School, Boston, MA, and approved August 30, 2016 (received for review April 27, 2016)

Phospholamban (PLN) plays a central role in Ca^{2+} homeostasis in cardiac myocytes through regulation of the sarco(endo)plasmic reticulum Ca^{2+}-ATPase 2A (SERCA2A) Ca^{2+} pump. An inherited mutation converting arginine residue 9 in PLN to cysteine (R9C) results in dilated cardiomyopathy (DCM) in humans and transgenic mice, but the downstream signaling defects leading to decompensation and heart failure are poorly understood. Here we used precision mass spectrometry to study the global phosphorylation dynamics of 1,887 cardiac phosphoproteins in early affected heart tissue in a transgenic R9C mouse model of DCM compared with wild-type littermates. Dysregulated phosphorylation sites were quantified after affinity capture and identification of 3,908 phosphopeptides from fractionated whole-heart homogenates. Global statistical enrichment analysis of the differential phosphoprotein patterns revealed selective perturbation of signaling pathways regulating cardiovascular activity in early stages of DCM. Strikingly, dysregulated signaling through the Notch-1 receptor, recently linked to cardiomyogenesis and embryonic cardiac stem cell development and differentiation but never directly implicated in DCM before, was a prominently perturbed pathway. We verified alterations in Notch-1 downstream components in early symptomatic R9C transgenic mouse cardiomyocytes compared with wild type by immunoblot analysis and confocal immunofluorescence microscopy. These data reveal unexpected connections between stress-regulated cell signaling networks, specific protein kinases, and downstream effectors essential for proper cardiac function.

phospholamban | proteomic | bioinformatics | heart disease | signaling

Cardiovascular diseases (CVDs) leading to systolic/diastolic heart failure (HF), such as hypertensive/diabetic heart disease, stroke, and vascular atherosclerosis, are leading causes of death in the developed world (1). Many CVDs are associated with genetic predispositions. For example, in humans, the arginine to cysteine (R9C) substitution in phospholamban (PLN) has been shown to result in dilated cardiomyopathy (DCM) presenting in adolescence, leading to rapid deterioration of heart function and premature death (2). However, the etiology and molecular mechanisms of progression of DCM and other CVDs leading to HF are complex and still poorly understood, further complicating clinical assessment and management. From a biological and clinical perspective, the identification and characterization of clinically relevant, potentially druggable, pathways driving the maladaptive response in affected heart tissue are key challenges to improved diagnostic and therapeutic tools for earlier detection and preventative treatment of both inherited and chronic CVDs.

Cardiac muscle contraction is controlled by Ca^{2+} flux and signaling relays, which are perturbed in HF. Internal stores of Ca^{2+} required for the proper functioning of cardiomyocytes (CMs) are normally maintained through the function of the sarco(endo)plasmic reticulum Ca^{2+}-ATPase 2 (SERCA2) (3), which is responsible for the sequestration of Ca^{2+} resulting in muscle relaxation. SERCA2 activity is regulated through a reversible inhibitory interaction with PLN, which can be relieved by phosphorylation of PLN by protein kinase A (PKA) or Ca^{2+}/calmodulin-dependent protein kinase II (CaMKII) (3).

Proteomic analyses have revealed changes in the abundance of other effector proteins in diverse biochemical pathways in DCM. Notably, shotgun proteomic analysis of membrane protein expression dynamics in heart microsomes isolated from mice overexpressing a superinhibitory (I40A) mutant of PLN revealed changes in G protein-coupled receptor-mediated pathways leading to activation of protein kinase C (PKC) (4). We previously reported quantitative changes in protein and cognate mRNA expression levels in cardiac ventricular tissue at different time points in the development of DCM in R9C-PLN mice representing clear clinical stages in the progression to HF (5). We showed that the latter maladaptive response was driven by elevated activity of MAPK signaling by the protein kinases p38 and JNK, in part through down-regulation of prosurvival microRNAs (6). However, the underlying upstream and downstream signaling events preceding HF were not fully explored.

In the present study, we report a systematic, large-scale quantitative phosphoproteomic analysis of dysregulated protein phosphorylation-dependent signaling occurring at the early symptomatic stages of DCM progression in whole hearts from R9C mutant mice compared with wild-type littermates.

Significance

The present study demonstrates the utility of global phosphoproteomic profiling of diseased cardiac tissue to identify signaling pathways and other biological processes disrupted in cardiomyopathy. Perturbed Notch-1 signaling was identified by bioinformatics analyses of phosphoprotein patterns present in affected cardiac tissue in a transgenic mouse model system of dilated cardiomyopathy and by complementary molecular biology and microscopy techniques. In addition, dozens of other disturbed signaling pathways offer an opportunity for novel therapeutic and/or diagnostic clinically applicable targets. Although this study was performed in mice, only minor adjustments to the experimental approach would be required for comparative analysis of analogous samples from human cardiac patients, potentially leading to even more clinically relevant data.

Author contributions: U.K., H.G., A.O.G., and A.E. designed research; U.K., H.G., D.B., J.C., C.A., R.I., and P.S. performed research; U.K., H.G., D.B., J.C., R.I., P.S., A.O.G., and A.E. analyzed data; and U.K., A.O.G., and A.E. wrote the paper.

The authors declare no conflict of interest.

This article is a PNAS Direct Submission.

Freely available online through the PNAS open access option.

Data deposition: All mass spectrometry results reported in this paper have been uploaded to PRIDE, https://www.ebi.ac.uk/pride/archive/ (accession no. PXD004810). PRIDE is a public data repository for proteomics data, including protein and peptide identifications, posttranslational modifications, and supporting spectral evidence. PRIDE is a core member in the ProteomeXchange (PX) consortium.

[1]U.K. and H.G. contributed equally to this work.

[2]To whom correspondence may be addressed. Email: anthony.gramolini@utoronto.ca or andrew.emili@utoronto.ca.

This article contains supporting information online at www.pnas.org/lookup/suppl/doi:10.1073/pnas.1606444113/-/DCSupplemental.

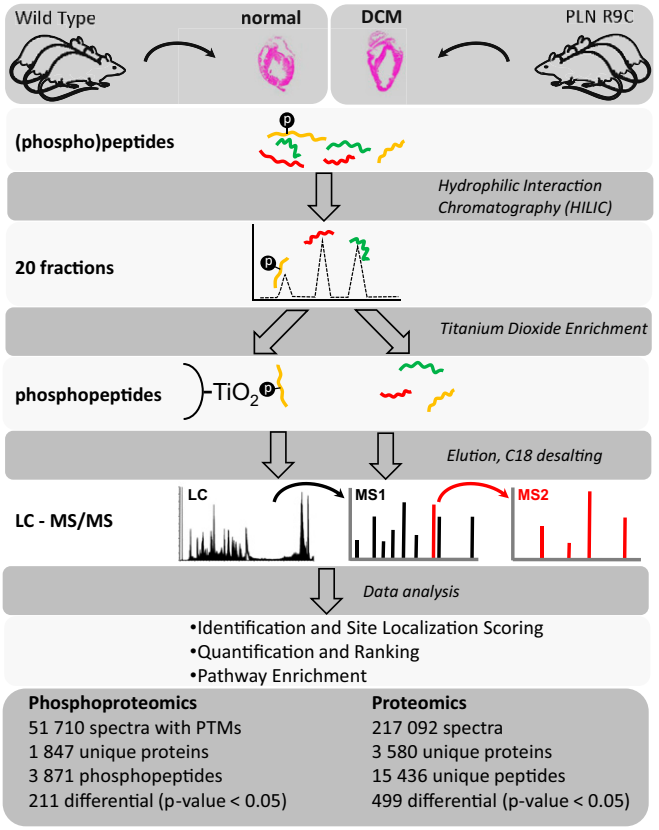

Fig. 1. General phosphoproteomics workflow. Three pooled hearts from R9C-PLN transgenic and wild-type littermates were analyzed by quantitative precision LC-MS/MS. PTM, posttranslational modification.

Results

Comparative Phosphoproteome Analysis. To achieve a comprehensive survey of cardiac signaling cascades impacted by DCM, we performed global quantitative phosphopeptide profiling on three independent biological replicates of whole-heart tissue isolated from 8-wk-old (early symptomatic) R9C mice and wild-type littermates (Fig. 1). A major experimental consideration was preservation of phosphorylation-site integrity, through use of phosphatase inhibitors, low temperature, and harsh denaturing sample-processing conditions. To achieve the deepest possible coverage, we performed chromatographic sample prefractionation steps, using hydrophilic interaction liquid chromatography to separate peptides bearing negatively charged phosphate moieties (7). Given the low relative abundance of phosphopeptides and their tendency to be undetectable due to ion competition/suppression during MS analysis, we performed differential affinity capture with immobilized metal oxide affinity chromatography (TiO_2) to enrich for phosphopeptides. To measure differences in relative abundance, we applied label-free quantification, comparing the extracted parent-ion current intensities recorded in high-energy collision dissociation (HCD) spectra using a high-precision orbitrap instrument. In parallel, we measured total protein levels by shotgun sequencing.

In total, our stringent data analysis workflow (Fig. S1) mapped 94,956 and 217,092 spectra to mouse reference protein sequences for the phosphoproteomic and background proteomic datasets, respectively. From this, we derived a set of high-confidence sequence matches [false discovery rate (FDR) ~1% at both protein and peptide levels] corresponding to over 1,800 cardiac phosphoproteins and 3,900 phosphopeptides in normal and DCM hearts, and 15,436 unique peptides mapping to 3,580 unique proteins in the background proteomic dataset (Fig. 2 *A* and *B*, Fig. S1, and Datasets S1–S3). For the former, we confidently (site-localization probability >0.7, as described in *SI Materials and Methods* and Datasets S4 and S5) identified 7,589 unique putative phosphorylation sites (i.e., sites on identified phosphopeptides with supporting MS/MS data and localization probability >0.7), of which 6,855 mapped to serine, 674 mapped to threonine, and 60 mapped to tyrosine residues (consistent with the expected 90:9:1 cellular distribution ratios) on 1,848 distinct cardiac proteins (Fig. 2 *A* and *B* and Datasets S1 and S2). Our coverage is comparable to a pioneering study of the mouse cardiac phosphoproteome by Lundby et al. (8) and a recent phosphoproteomic analysis of in vivo effects of CaMKII inhibition in mouse hearts (9). Phosphoproteins identified in our study also showed considerable overlap with heart and other tissue profiles in the mouse phosphoproteomic atlas reported by the Gygi group (10), but 333 were uniquely identified in our study, 96 of which contained phosphopeptides significantly altered and/or solely identified in R9C hearts (Fig. 2*C*). A high degree of overlap with the mouse ventricular myocyte proteome by Sharma et al. (11) was also observed (Fig. 2*D*).

Quantification and Ranking. Based on reproducible measurements of precursor-ion intensity, we scored both the individual phosphopeptides and their consolidated cognate phosphorylation sites for differential relative abundance between the healthy and diseased samples. Based on a two-tailed Student's *t* test ($P < 0.05$), the abundance of 211 phosphopeptides was differentially altered (elevated or reduced) between the R9C and WT hearts (Fig. 2*A* and Dataset S1), with 86% of these predominantly higher in the disease state. In comparison, 499 proteins showed differential expression, consistent with our previous report (5).

Systematic evaluation of the corresponding biological annotations revealed that the aberrant phosphorylation patterns occurred on proteins linked to disparate subcellular compartments, ranging from membrane-associated receptors to nuclear-localized proteins with established links to heart development, contractile function, and/or cardiomyopathy (Dataset S1). Consistent with expectation, the predominant phosphoform of PLN detected preferentially in R9C hearts was phosphorylated on serine 16, a site critical for inhibition of SERCA2 activity (3). We also detected alterations in the phosphorylation pattern of central kinases involved in cardiac

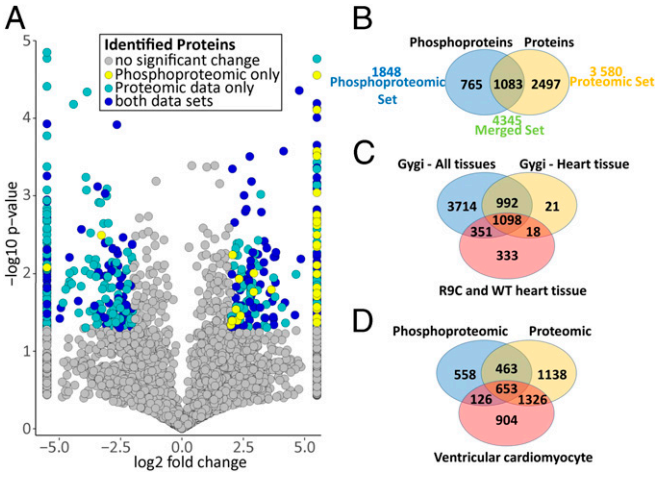

Fig. 2. (*A*) Volcano plot indicating significantly altered proteins and phosphoproteins identified in the combined datasets. Log-transformed *P* values (*t* test) associated with individual peptides and phosphopeptides plotted against log-transformed fold change in abundance between the R9C-PLN and wild-type hearts. (*B*) Venn diagram depicting the total number of proteins identified in the corresponding proteomic and phosphoproteomic datasets. (*C*) Venn diagram depicting phosphoprotein overlap with mouse tissue phosphoproteomes from Huttlin et al. (10). (*D*) Venn diagram depicting the overlap of the R9C and WT combined phosphoproteome and proteome with the ventricular cardiomyocyte proteome from Sharma et al. (11).

signaling such as PKA. Additionally, the S112 site on the PKA type II regulatory beta subunit (PRKAR2B), which results in the lowering of the activation threshold of PKA (12), increased in R9C. Additionally, we detected abundance changes in a cardiac stress marker (FHL1), an indicator of the fetal gene program (MYH7), markers of ECM remodeling (POSTN, SPARC), and proteins involved in Ca^{2+} modulation (SLMAP, CASQ2) (Datasets S1 and S2).

Further examples of interest include the highest-ranked phosphorylated peptide (S64 + T69) from eIF4E-binding protein 1 (EIF4EBP), which negatively regulates translation initiation. Hypophosphorylated EIF4EBP acts as a repressor of eIF4E whereas its phosphorylation releases eIF4E, thereby up-regulating protein translation in response to signaling by diverse cell-surface receptors, including insulin, EGF, PDGF, and other ligands (13). In heart, EIF4EBP has been implicated in ischemia–reperfusion stress, cardiomyocyte survival, cardiac hypertrophy, and oxidative and nutritional stress responses (13).

Also significantly more highly phosphorylated in R9C hearts was a previously uncharacterized T187 site in EMMPRIN (BSG/CD147), an extracellular metalloprotease-inducing member of the Ig superfamily, consistent with its role in inflammatory processes in cardiac remodeling (14). In addition, the S2 phosphosite on transcription factor MAX (Myc-associated factor X) (15), a positive regulator of cardiac alpha-myosin heavy-chain gene expression in cardiomyocytes, was significantly altered in R9C mice. Phosphorylation of S2 inhibits DNA binding by MAX homodimers and association with MYC but is not known to affect its interaction with another cofactor, transcription enhancer factor 1 (TEF-1, TEAD1), or regulation of cardiac alpha-myosin heavy chain (16). In contrast, when phosphorylated, the S73 site of transcription factor JUN, likewise more highly phosphorylated in the R9C mutant mice, is linked to increased transcription of JUN target genes encoding components of a myriad of signaling pathways (17).

Phosphosites on two intercalated disk-associated Xin repeat proteins (XIRP1, XIRP2) with roles in cardiac development were also increased significantly in R9C hearts. XIRPs interact with catenins and ion channels in mature cardiac muscle and, although the significance of phosphorylation is unclear, gene knockout mice display early-onset cardiomyopathy (18).

Kinase Target Motif Analysis. We used the MotifX algorithm (19) to identify consensus motifs overrepresented in the set of phosphopeptides identified exclusively in R9C heart tissue and/or those showing significant ($P < 0.05$) differential expression between R9C and wild-type mice (Table 1 and Dataset S1). Candidate consensus sequences were processed using PhosphoMotif Finder (20) to identify cognate kinases known or predicted to phosphorylate these sequences.

We found central kinases involved in cardiac contractility through transient Ca^{2+} regulation among the most overrepresented compared with the whole mouse proteome. Two consensus motifs identified were targeted by PKA and CaMKII (Table 1), one enriched 4.76-fold (59 matches) over background and the other 5.64-fold (34 matches). Phosphorylation of PLN by PKA on S16, or by CaMKII on T17, reverses PLN-mediated inhibition of SERCA2a activity up to 3-fold during β-adrenergic stimulation (3). Up-regulation of these kinases is expected as a compensatory mechanism considering that R9C-PLN mutant molecules effectively trap PKA, inhibiting phosphorylation of wild-type protein and relieving SERCA2a inhibition (2).

Two consensus sequences targeted by extracellular signal-regulated kinases (ERK1/2) were identified on 275 significantly altered phosphopeptides (Table 1). ERK1/2 become activated in cardiac myocytes in response to a variety of stimuli, including progression of DCM (21). Likewise, we found consensus motifs associated with phosphorylation by casein kinases and GSK3 kinases, previously linked to cardiac pathology (22).

Pathway Network Enrichment Analysis. For each phosphoprotein (and corresponding gene), the most differential peptide or modification site was selected for a systematic pathway enrichment analysis (*SI Materials and Methods*). Phosphopeptides were initially ranked based on the level of statistical significance (differential P value) rather than direction (up/down) of observed fold change. The focus of this analysis was to identify pathway-level alterations present in R9C mice compared with controls.

Three sets of enrichment analyses were performed to gain the most complete coverage, based on ranking (*i*) the phosphoproteomic dataset alone, (*ii*) the background proteomic dataset alone, and (*iii*) a merged combination of both (Fig. 2 *A* and *B* and Fig. S1), which included the significant differentially abundant proteins derived from both the proteomic background and differential phosphorylation events. This merged set of 4,345 unique proteins/genes (Fig. 2*B*) was included because signaling perturbations do not necessarily consist only of changes in phosphorylation state or protein expression alone but often rather both in concert. The most differentially expressed peptides or phosphorylation events (based on P value) from each protein were used to represent individual protein/gene products. The majority of enriched pathways found in the merged set (Dataset S3) reflected the presence of many proteins exclusively in the background proteome. Of the 2,039 gene sets enriched in the merged set, many (1,427) were likewise enriched in the global proteomic data alone (Fig. S1).

We chose to focus on a subset of 612 pathways and processes that reflected contributions from both datasets, rather than merely differential protein levels. To simplify analysis by minimizing redundancy in the annotation term labels (Dataset S1), we combined the 182 enrichments from the phosphoproteomic dataset (not in the background proteome) with the 526 gene sets unique to the merged set (Fig. S1 and Dataset S3). By visualizing the resulting 708 enriched gene sets as a single graphical enrichment map (23) (Dataset S6), we identified several dysregulated

Table 1. Top 10 ranked identified consensus motifs on phosphopeptides significantly altered and/or exclusively detected in R9C heart tissue with kinases predicted to target these sequences

Motifs	Kinase	Motif score	Matches	Fold increase
...RS.S.....	CamKII, PKA, PKC, CK2	27.34	59	4.76
.....SD.E...	CK2	24.66	34	6.77
....SPT.....	GSK3, ERK1/2, CDK5, CK2, DNA-PKCs	23.7	27	7.75
.R..S.S.....	CamK2, PKA, PKC, CK2	23.62	34	5.64
....SDS.....	CK2, BARK	17.65	21	6.41
.....SP....	GSK3, ERK1/2, CDK5	16	275	2.34
...S..S.....	CK1/2	16	258	1.74
...R..S.....	CamK2, PKA, PKC	12.45	123	2.01
.....TP.....	GSK3, ERK1/2, CDK5	9.46	63	2.35
..S...S.....	GPCRK1, MAPKAPK2K, GSK3	8.1	120	1.7

The number of matches in the query set and the fold increase over the normal occurrence of consensus sequence are also provided.

pathways of notable relevance to cardiac pathology (Table 2 and Fig. S2). For instance, reflecting a central role in cardiac physiology and pathology, dysregulated pathways associated with activation PKA- and cAMP-dependent kinases were prominently overrepresented in all gene set enrichment analyses (Datasets S1 and S3). Considering the ubiquity of many signaling pathways across different tissues and cell types, when examined as a whole (rather than individual components) it is not surprising that most pathways have associations with other disorders or processes. This is also partly a bias of existing annotations in curation databases.

To identify disease signatures specifically relevant to DCM, we integrated and compared these pathways against a recent in-depth RNA sequencing-based gene expression study of the R9C-PLN model (Datasets S2 and S7) (24). Specifically, differential mRNA expression modules in the Seidman study (24) corresponding to cardiomyocyte and nonmyocyte cardiac cell populations at different stages of disease (represented by six individual nodes) were tested for overlap with our enrichment map using a stringent Mann–Whitney test cutoff ($P < 0.01$). Strikingly, we observed highly significant overlap between most of the disrupted biological processes and signaling pathways noted by the two studies, including (but not limited to) innate immunity, glucose metabolism, TGF-β signaling, PPAR signaling, Wnt/β-catenin signaling, and TLR signaling (Dataset S8). Notably, the general pathways involved in metabolic and profibrotic processes determined by the Seidman study to differentiate between DCM and hypertrophic cardiomyopathy (HCM) were likewise detected as differentially perturbed in R9C hearts in our merged data.

Notch-1 Signaling. Distinct from the Seidman study, however, we identified evidence for significant disruption in homeostatic Notch-1 signaling in R9C hearts, with most phosphosites never reported before in the context of DCM. For instance, uncharacterized sites on SNW1 and CREBBP, members of the Notch-1 transcription coactivator complex (25), were hyperphosphorylated in the R9C mice. Similarly, we detected previously unreported phosphorylation sites on both MAX and NCOR1/2, components of a downstream transcriptional corepressor complex known to inhibit transcription of Notch target genes (26).

To directly determine the differential state of Notch receptor signaling, we performed immunoblots (Fig. 3*A*) using a panel of antibodies targeting different Notch receptor isoforms (Notch1/3), activating and inhibiting ligands (DLL1/4, JAGG1/2, NUMB), processing enzymes (ADAM9/17), and key downstream effector transcription factors (HEY2, HES3, SOX9). Strikingly, a very substantive and specific decrease in total Notch-1 receptor levels was seen in the R9C hearts, whereas levels of Notch-3 receptor were unchanged (Notch-2 was undetectable, as was the cleaved Notch-1 intracellular domain).

Of the activating Notch ligands, DLL1 was down-regulated in R9C whereas JAGG1 showed no change (DLL4 and JAGG2 were not detected). Conversely, DLL3 and NUMB, which can

Table 2. List of select cardiac-relevant signaling pathways, from the gene set enrichment analysis, along with their relevant protein components, altered in R9C-PLN hearts

Pathway	Identified components	Cardiac context
Notch-1 signaling	**hdac7(s178)**, **tle3(s216)**, **snw1(s224,s232)**, **tmed2**, **ncor2**,* **tbl1xr1**, **tbl1x**, ncor1(s2351), ep300, adam10, crebbp, rbx1, numb, hdac5(s652), arrb1, rps27a, mib1	Dilated cardiomyopathy, left ventricular noncompaction, cardiac development (36, 40)
VIP signaling	**map3k1(s915)**, **ppp3cb(s469)**, **plcg1(s1263)**, **nfatc2(s136)**, **prkar2b(s112)**, **prkacb**, prkar2a, prkar1a, nfkb1, ppp3ca	Myocardial fibrosis, diabetic cardiomyopathy, ischemia–reperfusion (41)
H3-K4 histone methylation	**ogt**, **kmt2a**, **snw1(s224,s232)**, **nipbl(s2652)**, **bcor(s423)**, **men1**, **kdm1a**, **mt2b**, **dnmt1**,* pml(s449), pygo2(t264), ctbp1, arrb1, ube2n, wbp2, lpin1	Hypertrophic cardiomyopathy, fetal gene program (42)
BCR signaling, beta-cell activation and regulation	**mif**, **irs2(s1165)**, **thoc1(s560)**, **sos1**,* **orai1**, **fas**,* **sash3**,* **ptprc(s801)**, **lyn(s19)**, **syk**, **itpr1(s1573)**, **cd81**, **stim1**,* **ptpn6**, **nfatc2(s136)**, **inpp5d(t701, s709)**, **sh3kbp1(s193)**, **aplf(s41)**, **cbl**, **plcg1(s1263)**, **tcf3(s517)**, **bad(s112)**, **itpr2**, calm1, pawr, itpr3, bmi1, nck1	Heart failure, hypertrophy, myocardial fibrosis, myocardial infarction, ischemia–reperfusion (43, 44)
TGF-β/smad signaling	**glg1**, **pdpk1(s117)**, **jun(s63)**, **lemd3**, **fbn2**, **men1**, **zeb1**, **aspn**, **eng**, **snx6**, zfyve9, cav3, sptbn1, bcl9l, strap, cav2,* ppm1a, htra1	Dilated cardiomyopathy, heart failure, fibrosis, myocardial infarction, cardiac remodeling (24, 45)
PPAR-α signaling	**med19(s226)**, **txnrd1**, **ankrd1**, **wwtr1**,* **abca1(s2234)**, **yap1**, **med24**,* **tbl1xr1**, **alas1**, **cdk19**, **tbl1x**, apoa1, acox1, apoa2, smarcd3, agt, ncoa3,* ncoa2, nfya(s187), fhl2, sp1, ncoa6, acadm, acsl1, cd36, crebbp, slc27a1, cpt2, ncor1(s2351), plin2, me1, ep300	Dilated cardiomyopathy, heart failure, diabetic cardiomyopathy (24, 46)
TLR signaling	**hsp90b1(s306)**, **lgmn**, **ikbkb**, **map2k1**, **app**, **nfkb2(t425)**, **dhx9(s137)**, **dnm2**, **ppp2r5d**,* **unc93b1**, **dnm1(s774)**, **itgb2**, **rps6ka3**, **eea1**, dusp3, tlr3, ctsb, nfkb1, ube2n, ppp2ca, cd36, mef2a, ppp2r1a	Dilated cardiomyopathy, heart failure, ischemia–reperfusion, hypertrophy, viral myocarditis (24, 47)
Wnt signaling	**scyl2(s253)**, **dab2ip(s854)**, **ranbp3**, **cdh2**, **wwtr1**,* **rapgef1**,* **gsk3a**, **ppp2r3a**, **mcc**,* **dab2**, **limd1**, **ctnnb1**, **dact3(s165)**, **bicc1**, **gsk3b**, **stk3(s246)**, **ctnnd1(s813)**, **g3bp1**, cav1, ppp2r5a, pi4k2a(s462), cul3, mapk14,* dvl3,* hdac2(s394)	Dilated cardiomyopathy, fibrosis, heart failure, myocardial infarction, arrhythmia (24, 48)

Phosphopeptides/proteins increased in R9C hearts are shown in bold, whereas components identified but showing a decrease in R9C are not bolded. The identified phosphorylation site of a particular protein is indicated in parentheses. For a full list of protein/gene names associated with each pathway, refer to Datasets S1–S3.
*Proteins annotated as "ambiguous," as described in *SI Materials and Methods*.

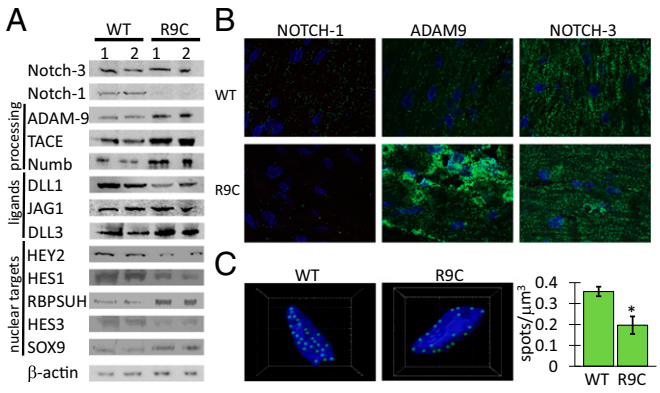

Fig. 3. (*A*) Immunoblots of components of the Notch-1 signaling pathway. (*B*) Immunofluorescence images of Notch-1, ADAM9, and Notch-3 in ventricular sections of WT and R9C-PLN hearts. (*C*) Representative reconstructed images showing nuclear localization of the Notch-1 intracellular domain and a bar graph showing quantification of relative distribution (spots identified/nuclear volume as determined by Hoechst staining) in WT and R9C-PLN hearts (mean ± SEM, $*P = 0.00282$).

suppress Notch signaling, were up-regulated in R9C hearts. Two metalloproteinases (ADAM9 and TACE/ADAM17) required for extracellular processing and/or degradation of the Notch-1 receptor were similarly up-regulated in R9C. Conversely, the downstream Notch-1–regulated transcription factors HES1 and HEY2 were down-regulated in R9C.

Immunofluorescence visualization of components of the Notch signaling pathway in the ventricular wall of R9C and wild-type hearts (Fig. 3*B*) established down-regulation of Notch-1 receptor expression in R9C cardiomyocytes along with up-regulation of the ADAM9 metalloproteinase (Notch-3 was unchanged). Imaris-based quantification (Fig. 3*C*) of signal intensity and localization of the Notch-1 intracellular domain (N1CID) in cardiomyocyte nuclei, indicative of Notch-1 activation, revealed a significant decrease ($P < 0.003$) in overall nuclear localization of N1CID in cells in the ventricular sections of R9C hearts compared with controls (due to gross changes in tissue morphology in R9C hearts, a large proportion of nuclei showed no N1CID colocalization). These results verify Notch-1 receptor signaling inhibition in affected heart tissue during early-stage disease (Fig. 4).

Discussion

During pathological cardiac remodeling, including DCM, disruptions in various signaling cascades have been reported, including AKT, ERKs, GSK3, JAKs, MAPKs, PI3K, PKA, PKC, and TGF-β. Activation or inhibition of signaling pathways can ultimately result in changes to cardiomyocyte cell growth, differentiation, proliferation, and/or survival (27). However, despite advances in understanding the molecular basis of cardiac disease, a clear global picture of system-wide signaling network perturbations does not exist for most conditions, including DCM. To address this gap, we applied quantitative precision mass spectrometry to glean the complex interplay of signaling events associated early during disease progression with a genetic cause of cardiac HF.

One-third of all cardiac proteins are known or predicted to be phosphorylated. Here, we mapped 7,589 phosphopeptides on 1,848 cardiac proteins, of which 211 were differentially abundant in the R9C model, providing unprecedented insights into the global dysregulation of signaling cascades in early-stage DCM. Many sites we identified are novel and of unknown biological significance. Although annotated repositories of experimental phosphoproteomic datasets have been established (e.g., PhosphoSitePlus) (28), establishing relevance to heart biology and CVD is not straightforward. Our present study aimed to first identify significantly altered individual phosphosites and then use the corresponding associated protein/gene annotations in conjunction with information gained from global proteomic analysis. This design was motivated by computational tools for signaling network analysis and visualization, which historically focused on gene expression datasets rather than individual phosphosites.

One especially intriguing finding was identification of Notch-1 signaling as prominently altered in DCM. The Notch pathway is a widely studied system crucial to "cell-fate" determination (29). Mammals express four Notch receptors (Notch-1 to Notch-4) and five ligands (DLL1/3/4, JAGG1/2) (30). Notch-1 is expressed across a broad variety of cell types, including cardiomyocytes. All members of the Notch family are translated as single chains but are subsequently processed in the Golgi system to produce extracellular and transmembrane subunits that remain bound together at the plasma membrane by noncovalent bonds. Generally, ligand binding triggers the selective cleavage and removal of the extracellular subunit by members of the ADAM protease family, followed by cleavage of the membrane-bound intracellular subunit by γ-secretase to release N1ICD, which translocates to the nucleus to modulate transcription (Fig. 4). However, this oversimplification does not reflect cell context, as different ligands can act as Notch inhibitors whereas processing enzymes can oppose Notch activation (29).

Changes in phosphorylation of Notch signaling components included an uncharacterized phosphorylation site on the polyubiquitin protein UBB required for homeostatic recycling of Notch-1, which is up-regulated in R9C mice (31), as well as members of the histone deacetylase family (HDAC4/7/9) and others (32). However, due to incomplete functional annotation, our cautious conclusion was that the Notch-1 pathway was disrupted but not the precise nature of the perturbation (i.e., activation/inhibition).

We verified changes in Notch-1 signaling by immunoblotting and immunofluorescence. We demonstrated down-regulation of Notch-1 and DLL1 in R9C. DLL3, a Notch-1 ligand previously shown to be a *cis*-acting inhibitor (33), was up-regulated along with NUMB, whose association with Notch-1 leads to proteasomal degradation (34). ADAM9 and TACE/ADAM17, normally necessary for activation of Notch-1, were also up-regulated in R9C. However, excessive expression of these proteases has also been shown to inhibit Notch signaling, whereas deficiency of a major associated inhibitor, TIMP3, leads to dilated cardiomyopathy in mice (35). Furthermore, expression and nuclear localization of the N1ICD domain of Notch-1 were significantly greater in wild-type cardiomyocytes compared with R9C. Together, these results show that Notch-1 signaling is down-regulated in myocardium in early-stage DCM.

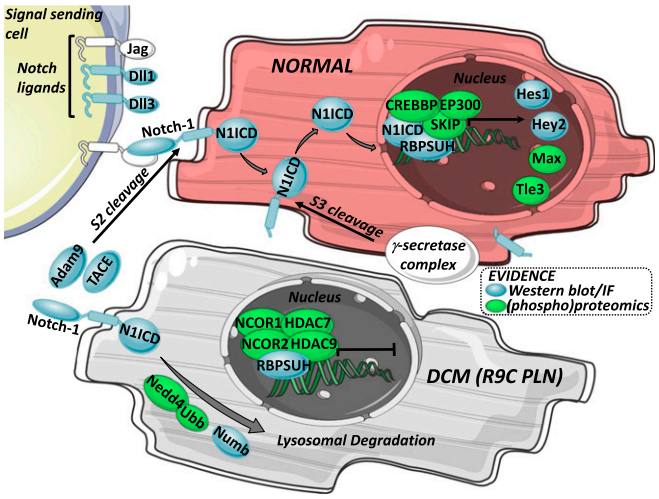

Fig. 4. Proposed schematic model of Notch-1 signaling in normal and DCM cardiomyocytes populated with differential proteins identified with different lines of evidence in whole-heart lysates or ventricular sections, including proteomic data, phosphoproteomic data, immunoblotting, and immunofluorescence (IF).

Our findings are consistent with previous reports of development of DCM in vitro and in newborn mice treated with an inhibitor of Notch-1–dependent signaling (36), or more pronounced cardiac dysfunction, fibrosis, and apoptosis in adult hearts from an agonist-induced hypertrophy model or Notch-1 cardiac-specific null mice (37). Similarly, transgenic mice overexpressing the Notch ligand JAGGED1 were protected from pressure overload-induced cardiac hypertrophy (38).

Considering these unprecedented phosphoproteomics data, it is clear that a more complete understanding of Notch-1 signaling and other potentially relevant pathways in adult heart following injury, including in human patients, is warranted (39). Indeed, uncoupling of Notch-1 signaling in R9C (Fig. 4) suggests that Notch-1–activating compounds (i.e., activating antibodies, polypeptides, small molecules) may be clinically beneficial under DCM conditions, similar to that observed in hypertrophy (38) and potentially other pathological contexts.

Materials and Methods

Transgenic mice carrying the R9C mutation in the PLN gene were previously described (2) and experiments were approved by the Animal Use Committee at the University of Toronto. Workflows for heart sample preparation, processing, and (phospho)proteomic profiling, including chromatographic fractionation, MS data generation, phosphosite localization and scoring, statistical enrichment analyses, motif prediction, Western blotting, and immunofluorescence, are detailed in *SI Materials and Methods* and Table S1.

ACKNOWLEDGMENTS. We thank Paul Taylor, Peter Backx, Gary Bader, Michael Moran, and David H. MacLennan for valuable advice. This project was funded by the Heart and Stroke Foundation of Ontario (T-6281; to A.O.G.), Canadian Institutes of Health Research (MOP-106538; to A.O.G.), Ontario Research Fund (Global Leadership in Genomics and Life Sciences Grant GL2-01012), and Heart and Stroke Richard Lewar Centre (A.O.G. and A.E.). A.O.G. is a Canada Research Chair in Cardiovascular Proteomics and Molecular Therapeutics. A.E. is the Ontario Research Chair in Biomarkers of Disease Management. U.K. received postdoctoral fellowship support from the Ted Rogers Centre for Heart Research.

1. Mozaffarian D, et al.; American Heart Association Statistics Committee and Stroke Statistics Subcommittee (2015) Heart disease and stroke statistics—2015 update: A report from the American Heart Association. *Circulation* 131(4):e29–e322.
2. Schmitt JP, et al. (2003) Dilated cardiomyopathy and heart failure caused by a mutation in phospholamban. *Science* 299(5611):1410–1413.
3. MacLennan DH, Kranias EG (2003) Phospholamban: A crucial regulator of cardiac contractility. *Nat Rev Mol Cell Biol* 4(7):566–577.
4. Pan Y, et al. (2004) Identification of biochemical adaptations in hyper- or hypocontractile hearts from phospholamban mutant mice by expression proteomics. *Proc Natl Acad Sci USA* 101(8):2241–2246.
5. Gramolini AO, et al. (2008) Comparative proteomics profiling of a phospholamban mutant mouse model of dilated cardiomyopathy reveals progressive intracellular stress responses. *Mol Cell Proteomics* 7(3):519–533.
6. Isserlin R, et al. (2015) Systems analysis reveals down-regulation of a network of pro-survival miRNAs drives the apoptotic response in dilated cardiomyopathy. *Mol Biosyst* 11(1):239–251.
7. Engholm-Keller K, Larsen MR (2013) Technologies and challenges in large-scale phosphoproteomics. *Proteomics* 13(6):910–931.
8. Lundby A, et al. (2013) In vivo phosphoproteomics analysis reveals the cardiac targets of β-adrenergic receptor signaling. *Sci Signal* 6(278):rs11.
9. Scholten A, et al. (2013) Phosphoproteomics study based on in vivo inhibition reveals sites of calmodulin-dependent protein kinase II regulation in the heart. *J Am Heart Assoc* 2(4):e000318.
10. Huttlin EL, et al. (2010) A tissue-specific atlas of mouse protein phosphorylation and expression. *Cell* 143(7):1174–1189.
11. Sharma P, et al. (2015) Evolutionarily conserved intercalated disc protein Tmem65 regulates cardiac conduction and connexin 43 function. *Nat Commun* 6:8391.
12. Terrin A, et al. (2012) PKA and PDE4D3 anchoring to AKAP9 provides distinct regulation of cAMP signals at the centrosome. *J Cell Biol* 198(4):607–621.
13. Vary TC, Lang CH (2008) Differential phosphorylation of translation initiation regulators 4EBP1, S6k1, and Erk 1/2 following inhibition of alcohol metabolism in mouse heart. *Cardiovasc Toxicol* 8(1):23–32.
14. Venkatesan B, et al. (2010) EMMPRIN activates multiple transcription factors in cardiomyocytes, and induces interleukin-18 expression via Rac1-dependent PI3K/Akt/IKK/NF-kappaB andMKK7/JNK/AP-1 signaling. *J Mol Cell Cardiol* 49(4):655–663.
15. Bousset K, Henriksson M, Lüscher-Firzlaff JM, Litchfield DW, Lüscher B (1993) Identification of casein kinase II phosphorylation sites in Max: Effects on DNA-binding kinetics of Max homo- and Myc/Max heterodimers. *Oncogene* 8(12):3211–3220.
16. Gupta MP, Amin CS, Gupta M, Hay N, Zak R (1997) Transcription enhancer factor 1 interacts with a basic helix-loop-helix zipper protein, Max, for positive regulation of cardiac alpha-myosin heavy-chain gene expression. *Mol Cell Biol* 17(7):3924–3936.
17. Karin M, Gallagher E (2005) From JNK to pay dirt: Jun kinases, their biochemistry, physiology and clinical importance. *IUBMB Life* 57(4–5):283–295.
18. Wang Q, Lin JL, Chan SY, Lin JJ (2013) The Xin repeat-containing protein, mXinβ, initiates the maturation of the intercalated discs during postnatal heart development. *Dev Biol* 374(2):264–280.
19. Chou MF, Schwartz D (2011) Using the scan-x web site to predict protein post-translational modifications. *Curr Protoc Bioinformatics* Chapter 13:Unit 13.16.
20. Keshava Prasad TS, et al. (2009) Human Protein Reference Database—2009 update. *Nucleic Acids Res* 37(Database issue):D767–D772.
21. Wang Y (2007) Mitogen-activated protein kinases in heart development and diseases. *Circulation* 116(12):1413–1423.
22. Juhaszova M, et al. (2009) Role of glycogen synthase kinase-3beta in cardioprotection. *Circ Res* 104(11):1240–1252.
23. Isserlin R, Merico D, Voisin V, Bader GD (2014) Enrichment Map—A Cytoscape app to visualize and explore OMICs pathway enrichment results. *F1000Res* 3:141.
24. Burke MA, et al. (2016) Molecular profiling of dilated cardiomyopathy that progresses to heart failure. *JCI Insight* 1(6):e86898.
25. Zhou S, et al. (2000) SKIP, a CBF1-associated protein, interacts with the ankyrin repeat domain of NotchIC to facilitate NotchIC function. *Mol Cell Biol* 20(7):2400–2410.
26. Espinosa L, Santos S, Inglés-Esteve J, Muñoz-Canoves P, Bigas A (2002) p65-NFkappaB synergizes with Notch to activate transcription by triggering cytoplasmic translocation of the nuclear receptor corepressor N-CoR. *J Cell Sci* 115(Pt 6):1295–1303.
27. Sun Z, Hamilton KL, Reardon KF (2012) Phosphoproteomics and molecular cardiology: Techniques, applications and challenges. *J Mol Cell Cardiol* 53(3):354–368.
28. Ren J, et al. (2011) Computational analysis of phosphoproteomics: Progresses and perspectives. *Curr Protein Pept Sci* 12(7):591–601.
29. Morrisey EE (2010) Weary of the stress: Time to put another notch in cardiomyopathy. *Circ Res* 106(7):1187–1189.
30. Rizzo P, et al. (2015) The role of Notch in the cardiovascular system: Potential adverse effects of investigational Notch inhibitors. *Front Oncol* 4:384.
31. Ryu HW, Park CW, Ryu KY (2014) Disruption of polyubiquitin gene Ubb causes dysregulation of neural stem cell differentiation with premature gliogenesis. *Sci Rep* 4:7026.
32. Tang Y, Boucher JM, Liaw L (2012) Histone deacetylase activity selectively regulates Notch-mediated smooth muscle differentiation in human vascular cells. *J Am Heart Assoc* 1(3):e000901.
33. Chapman G, Sparrow DB, Kremmer E, Dunwoodie SL (2011) Notch inhibition by the ligand DELTA-LIKE 3 defines the mechanism of abnormal vertebral segmentation in spondylocostal dysostosis. *Hum Mol Genet* 20(5):905–916.
34. Wu M, Li J (2015) Numb family proteins: Novel players in cardiac morphogenesis and cardiac progenitor cell differentiation. *Biomol Concepts* 6(2):137–148.
35. Fedak PW, et al. (2006) Altered expression of disintegrin metalloproteinases and their inhibitor in human dilated cardiomyopathy. *Circulation* 113(2):238–245.
36. Urbanek K, et al. (2010) Inhibition of Notch1-dependent cardiomyogenesis leads to a dilated myopathy in the neonatal heart. *Circ Res* 107(3):429–441.
37. Croquelois A, et al. (2008) Control of the adaptive response of the heart to stress via the Notch1 receptor pathway. *J Exp Med* 205(13):3173–3185.
38. Metrich M, et al. (2015) Jagged1 intracellular domain-mediated inhibition of Notch1 signalling regulates cardiac homeostasis in the postnatal heart. *Cardiovasc Res* 108(1):74–86.
39. Gude N, Sussman M (2012) Notch signaling and cardiac repair. *J Mol Cell Cardiol* 52(6):1226–1232.
40. D'Amato G, Luxán G, de la Pompa JL (2016) Notch signalling in ventricular chamber development and cardiomyopathy. *FEBS J*, 10.1111/febs.13773.
41. Dvorakova MC, Kruzliak P, Rabkin SW (2014) Role of neuropeptides in cardiomyopathies. *Peptides* 61:1–6.
42. Zaidi S, et al. (2013) De novo mutations in histone-modifying genes in congenital heart disease. *Nature* 498(7453):220–223.
43. Cordero-Reyes AM, et al. (2016) Full expression of cardiomyopathy is partly dependent on B-cells: A pathway that involves cytokine activation, immunoglobulin deposition, and activation of apoptosis. *J Am Heart Assoc* 5(1):e002484.
44. Hofmann U, Frantz S (2015) Role of lymphocytes in myocardial injury, healing, and remodeling after myocardial infarction. *Circ Res* 116(2):354–367.
45. Dobaczewski M, Chen W, Frangogiannis NG (2011) Transforming growth factor (TGF)-β signaling in cardiac remodeling. *J Mol Cell Cardiol* 51(4):600–606.
46. Finck BN (2007) The PPAR regulatory system in cardiac physiology and disease. *Cardiovasc Res* 73(2):269–277.
47. Vallejo JG (2011) Role of Toll-like receptors in cardiovascular diseases. *Clin Sci (Lond)* 121(1):1–10.
48. Dawson K, Aflaki M, Nattel S (2013) Role of the Wnt-Frizzled system in cardiac pathophysiology: A rapidly developing, poorly understood area with enormous potential. *J Physiol* 591(6):1409–1432.
49. Beausoleil SA, Villén J, Gerber SA, Rush J, Gygi SP (2006) A probability-based approach for high-throughput protein phosphorylation analysis and site localization. *Nat Biotechnol* 24(10):1285–1292.
50. Chawade A, Alexandersson E, Levander F (2014) Normalyzer: A tool for rapid evaluation of normalization methods for omics data sets. *J Proteome Res* 13(6):3114–3120.
51. Schwartz D, Chou MF, Church GM (2009) Predicting protein post-translational modifications using meta-analysis of proteome scale data sets. *Mol Cell Proteomics* 8(2):365–379.